Catalytic and electrocatalytic behavior of Ni-based cermet anodes under internal dry reforming of $CH_4 + CO_2$ mixtures in SOFCs

G. Goula [a], V. Kiousis [a], L. Nalbandian [b], I.V. Yentekakis [a],*

[a] Department of Sciences, Technical University of Crete, 73100 Chania, Crete, Greece
[b] CPERI-CERTH, P.O.Box 361, 57001 Thermi, Thessaloniki, Greece

Abstract

A high temperature (700–900 °C) SOFC with yttria stabilized zirconia (YSZ) solid electrolyte was constructed and tested on direct feed of simulated biogas ($CH_4 + CO_2$) mixtures. Both catalytic, i.e. open-circuit, and electrocatalytic, i.e. closed-circuit, measurements were carried out. Open-circuit kinetic data showed that the rate of the catalytic reaction of the dry(CO_2)-reforming of methane is maximized at about equimolar CO_2/CH_4 feed ratio for all temperatures studied. Closed-circuit data showed that cell output characteristics (i.e. current and power densities) are also maximized for equimolar CO_2/CH_4 biogas composition. Power densities up to 51.6 mW/cm^2 (at $V = 453$ mV, $i = 114$ mA/cm^2, $T = 875$ °C) have been obtained. Long-term operation experiments demonstrated that the constructed biogas fuel cell has very stable behavior for all three different simulated biogas compositions fed, including poor, equimolar and rich methane constitutions.
© 2006 Elsevier B.V. All rights reserved.

1. Introduction

Methane and CO_2 are the main constituents of biogas, extensively produced today in an indigenous local base by anaerobic biological waste treatment [1–3]. Because of the different ways of production and the different waste sources, biogas composition varies significantly depending not only on different locations but also over time. Its composition usually lies within the following ranges: $CH_4 = (50–70\%)$, $CO_2 = (25–50\%)$, $H_2 = (1–5\%)$ and $N_2 = (0.3–3\%)$, with various minor impurities, notably NH_3, H_2S and halides [3]. Typical CO_2/CH_4 proportions are 40%/60%. At remarkably low levels of methane, conventional heat engines would not work [3], thus, poor-quality biogas is currently wasted by detrimental venting to the atmosphere. Methane is also the principal constituent of natural gas.

The reforming of methane by steam or CO_2, i.e.

$$CH_4 + H_2O \rightarrow CO + 3H_2 \tag{1}$$

$$CH_4 + CO_2 \rightarrow 2CO + 2H_2 \tag{2}$$

yielding H_2 and CO has received renewed interests today because of the possibility of enhancing natural gas valorization [4,5]. The reforming process can be considered as an inexpensive way of H_2 production but this is also the conventional industrial process for the production of synthesis gas (CO+H_2), which then can be used in the Fisher–Tropsch synthesis industry to produce valuable chemicals. Moreover, H_2, CO or H_2+CO mixtures produced by the reforming process can be used as efficient fuels for high temperature solid oxide fuel cells (SOFCs) to produce electricity [6].

Methane fuelled SOFC plants for electrical energy production often involve an external reformer, where methane is converted to CO and H_2 before these gases are supplied to the fuel cell compartment of the plant. Alternatively, the internal reforming

---

* Corresponding author. Fax: +30 28210 37843.
  E-mail address: yyentek@science.tuc.gr (I.V. Yentekakis).

concept has been considered as a more promising and advantageous design [6]. In this concept the reforming reaction takes place directly, without the necessity of an external reformer, onto the anodic electrode of the fuel cell, simultaneously with the charge transfer reactions that lead to electricity production [6]. Several investigations on fuel cells operating under internal reforming of methane have recently appeared in the literature (e.g. [7–10]). Although methane reforming can be performed by steam or CO_2, most of the internal reforming investigations have used steam as the reforming agent, while only few preliminary studies concern fuel cells operating under CO_2-reforming conditions [11].

In this work, an 8 mol% YSZ–SOFC of the type: $CH_4 + CO_2$, $Ni–YSZ$ $cermet/YSZ/La_xSr_{1-x}MnO_3$, air with a 65 wt.% Ni–YSZ cermet anode and a $La_{0.5}Sr_{0.5}MnO_3$ perovskite cathode was constructed in order to investigate its operation characteristics upon direct feed with simulated biogas mixtures. The feasibility of running this fuel cell at several biogas compositions including poor-quality biogases (low levels of CH_4), where conventional power generation systems present difficulties to operate [3], was also considered. At the anodic cell compartment, the internal dry reforming of CH_4 (reaction (2)) will be catalyzed onto the Ni electrode. Thus produced H_2 and CO can then be readily oxidized electrochemically at the three-phase-boundaries (tpb) Ni–YSZ–gas via the following charge transfer half reactions, to produce electricity:

$$H_2 + O^{2-} \rightarrow H_2O + 2e^- \qquad (3)$$

$$CO + O^{2-} \rightarrow CO_2 + 2e^- \qquad (4)$$

The kinetics of reactions (2)–(4) are fast at the operating temperatures of most SOFCs. Furthermore, reaction (2) is quite endothermic and thus its fast occurrence can cause severe cooling of the anode. Such a cooling can have a severe adverse effect on SOFC performance but it can, in principle, be balanced by a portion of the heat produced by the parallel exothermic reactions (3) and (4). The rest of the free energy change of these reactions concerns the electrical energy produced.

2. Experimental

The porous Ni–YSZ cermet anode was prepared by wet impregnation using the proper amounts of $Ni(NO_3)_2 6H_2O$ (Merck) and 8 mol% YSZ powder (Aldrich) as precursors. The solution was stirred at 80 °C until drying. Then it was slowly (5 °C/min) heated in air up to 800 °C for 20 min in order to decompose the nickel nitrate to NiO. The resulting powder was ball milled to reduce its grain size ($< \sim 5$ μm) and diluted in a small amount of water to form a viscous paste. In order to produce a Ni–YSZ electrode film from this cermet paste on the inside bottom wall of the YSZ tube, the paste was coated on the tube, dried and then progressively heated in air up to 1350 °C for 5 h. The total mass of the deposited anode was 36 mg with a superficial surface area of ~ 1.8 cm^2.

The perovskite electrode, i.e. the $La_{0.5}Sr_{0.5}MnO_3$ ceramic composite, was prepared by the citrate route method as described by Lamas et al. [12], using high purity La_2O_3, $MnCO_3$ and

$SrCO_3$ (Aldrich) as raw materials. The produced gel was slowly (2 °C/min) heated in air, kept for 1 h at 350 °C, and then sintered at 700 °C for 24 h to form the perovskite phase. In order to achieve a thin (~ 20 μm) perovskite electrode film onto the outside bottom wall of the YSZ tube, the perovskite powder was ball milled to reduce its grain size ($< \sim 5$ μm), diluted in alcohol, coated on the solid electrolyte wall, sintered in air up to 1000 °C at 5 °C/min and kept at the final temperature for 6 h.

The compositions of the synthesized anodic and cathodic electrodes were evaluated by ED-XRF analysis (PGT Model LS30143, 150 eV resolution at 5.9 keV). The morphology of the Ni–YSZ cermet electrode was examined by a JEOL 6300 SEM operated at accelerating voltage of 20 kV. Anodic and cathodic electrodes were also analyzed by XRD using a Siemens D500 X-ray diffractometer with an autodivergent slit and graphite monochromator using CuKα radiation.

The fuel cell reactor used consists of an 11 cm length YSZ tube closed flat at one end. The tube internal diameter is 1.6 cm, with a bottom wall thickness of 1 mm. The open end of the YSZ tube with the anodic and cathodic electrodes vis-a-vis deposited on its bottom walls was champed to an appropriately machined stainless-steel reactor cap with provisions for the introduction of the reactants and the removal of the products. The reactor appeared to be well mixed (CSTR) over a wide range of flow rates (10–300 cm^3/min) by obtaining the reactor residence time distribution with a mass spectrometer and using CO_2 as the inert tracer. Au lead wires were used to provide electrical connection with the inside anodic and outside cathodic electrodes; the constructed electrical circuit involves a voltmeter, an amperometer and a resistances box. The reactor cell was arranged onto an apparatus which involves cylinders with all the necessary gases, i.e. CO_2 (99.6%) and CH_4 (99.5%), ultra pure He, H_2 and 20% O_2 in He, and mass flow meters (MKS-247) to prepare the appropriate mixtures which were then fed to the cell. The analysis of the reactants and products involves on line G.C. (Shimadzu 14B) and Mass Spec. (Pfeiffer-Vacuum, Omnistar Prisma). The cell reactor and apparatus configurations are similar to those described in detail elsewhere [7] with the necessary modifications in order to fit the present circumstances. Before acquisition of open- or closed-circuit data the anode was activated by reduction in H_2 flow (10% H_2 diluted in He) at 850 °C for 30 min.

3. Results and discussion

3.1. Materials

Quantification of the XRF results, performed by comparison with appropriate available standards, gave a 61 wt.% of Ni for the Ni–YSZ cermet anode and a $La_{0.54}Sr_{0.46}MnO_3$ composition for the $La_xSr_{1-x}MnO_3$ perovskite cathode. These constitutions are satisfactorily close to those initially desired and based on the precursors mixed.

In Fig. 1 SEM images of the Ni–YSZ electrode film deposited onto the solid electrolyte wall, as described in the Experimental section, are shown. Image (a) corresponds to the Ni–YSZ film as it was initially deposited by the sintering method but before any other

treatment. Image (b) was taken after the reduction of the film with a flow of 10% H_2 (in He) at 850 °C for 30 min and then operated under dry reforming reaction conditions ($CO_2/CH_4 = 1/2$ at 850 °C for 30 min). In both cases the electrode film has a porous microstructure, while Ni and YSZ form two different phases. In the case of image (a) Ni is present as NiO crystals with diameters between 1–3 μm, while YSZ forms smooth spheroidal particles with diameters 0.5–2 μm. In the reduced film (b) the metallic phase is present in the form of particles with diameters 1–3 μm, which look darker and coarse and can be clearly distinguished from the smooth YSZ particles which remain unchanged compared to the unreduced sample (a). Both micrographs indicate good connection of Ni and
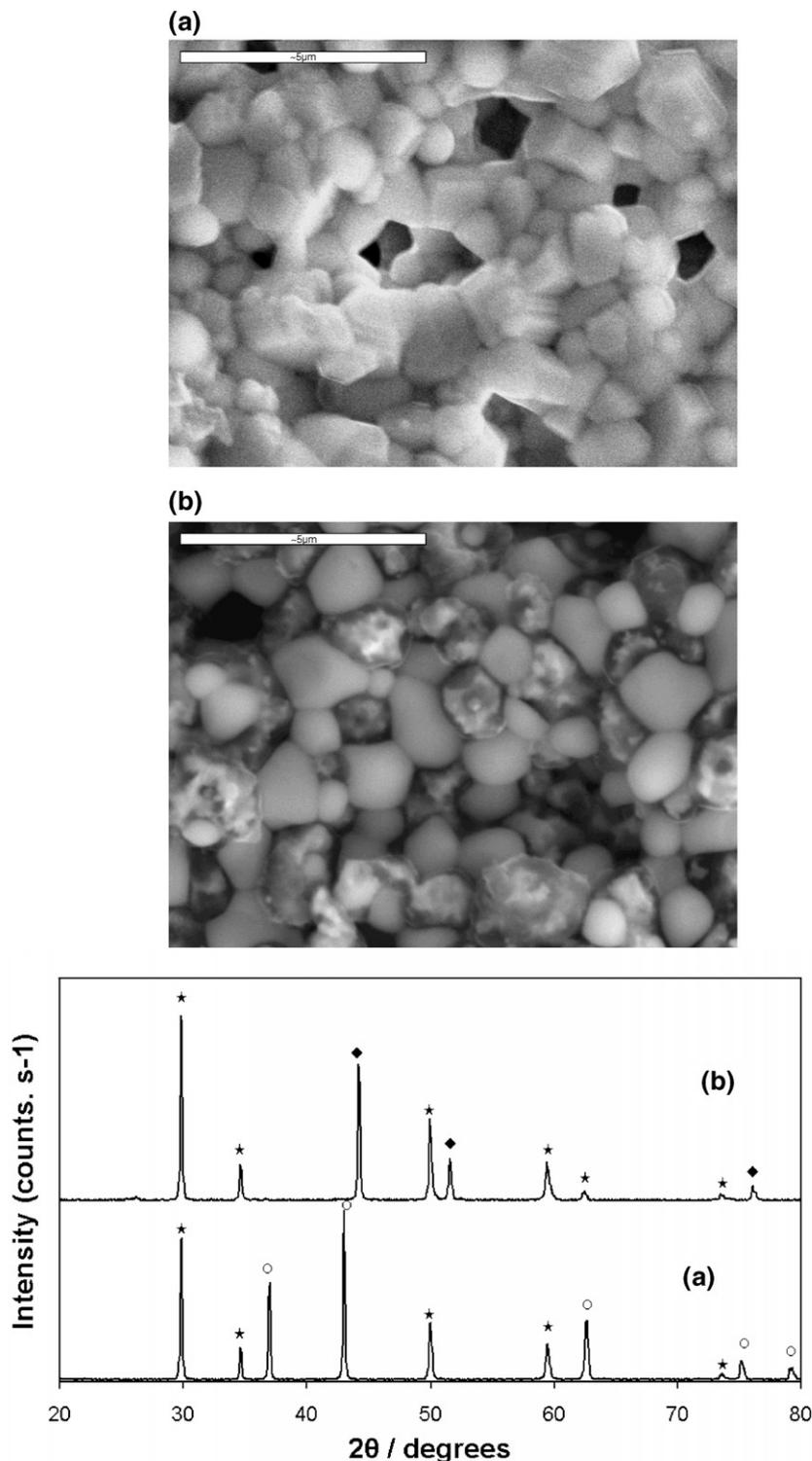
Fig. 1. SEM micrographs and the corresponding XRD patterns of the Ni–YSZ electrode film, before (a), and after reduction in H_2 flow and operated at CO_2-reforming reaction conditions (b). See text for discussion. Symbols: ○: NiO, ♂: Ni, ★: YSZ.

YSZ grains. Fig. 1 also depicts the XRD patterns, corresponding to cases (a) and (b). The patterns show that the reduction treatment converts almost completely NiO to Ni; the latter is very active to CO_2-reforming of methane catalysis contrary to NiO which was found to be practically inactive.

3.2. CO_2-reforming kinetics (open-circuit data)

Fig. 2 shows open-circuit kinetic data of the CO_2-reforming of methane over the Ni–YSZ cermet catalyst in a wide range of temperatures (600–900 °C) and CH_4 partial pressures (0.5–17 kPa) at constant partial pressure of CO_2 (5 kPa), thus covering a wide range of CO_2/CH_4 molar ratios into the reactor. Ultra pure He was used as diluting agent to keep the total pressure in the reactor at 1 bar. In all kinetic experiments the total conversions of CH_4 and CO_2 were kept below ∼20% to ensure that true kinetics are observed, which are not obscured by thermodynamic or mass transfer limitations. This is the reason of using diluted CH_4 and CO_2 gases and relatively high total flow rates (∼180 cm^3/min) for the data depicted in Fig. 2. The first interesting feature of Fig. 2 is that the methane consumption rate passes through a maximum for all temperatures investigated by varying P_{CH_4} (at constant P_{CO_2}). Forward and backward repetition cycles from low to high P_{CH_4} and vise versa did not give hysteresis phenomena; the reproducibility of the kinetics data was perfectly good. This reasonably implies that rate maxima do not reflect deactivation of the anode at low CO_2/CH_4 ratios (<1) due to extensive carbon deposition, which practically seems to be negligible at least for the time scale of the kinetic experiments; kinetics rather than deactivation phenomena may govern the appearance of rate maxima. This behavior strongly indicates competitive adsorption of CH_4 and CO_2 on the Ni surface, implying that the kinetics of CO_2-reforming of CH_4 on Ni catalyst can be modeled within the framework of classical Langmuir–Hinshelwood kinetics. Rate maxima are located at about equimolar CO_2/CH_4 composition for all temperatures investigated, which implies similar adsorption strengths for both reactants at 700–900 °C. Maximization of the rate of the reforming
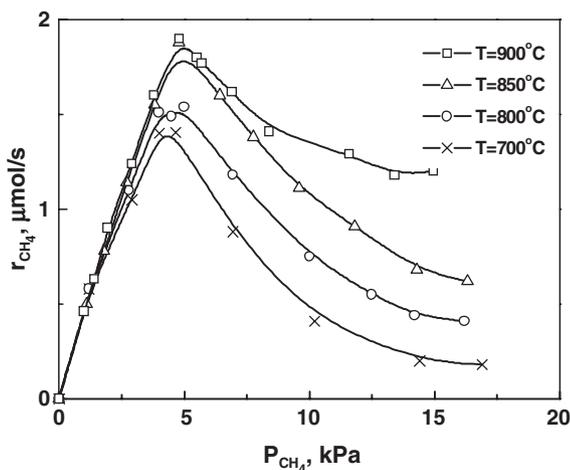
Fig. 2. CH_4 consumption rate during the internal dry-reforming reaction over the Ni–YSZ catalyst electrode as a function of the CH_4 partial pressure (P_{CH4}) at constant partial pressure of CO_2, P_{CO_2} = 5 kPa. Total flow rate F = 180 cm^3/min.
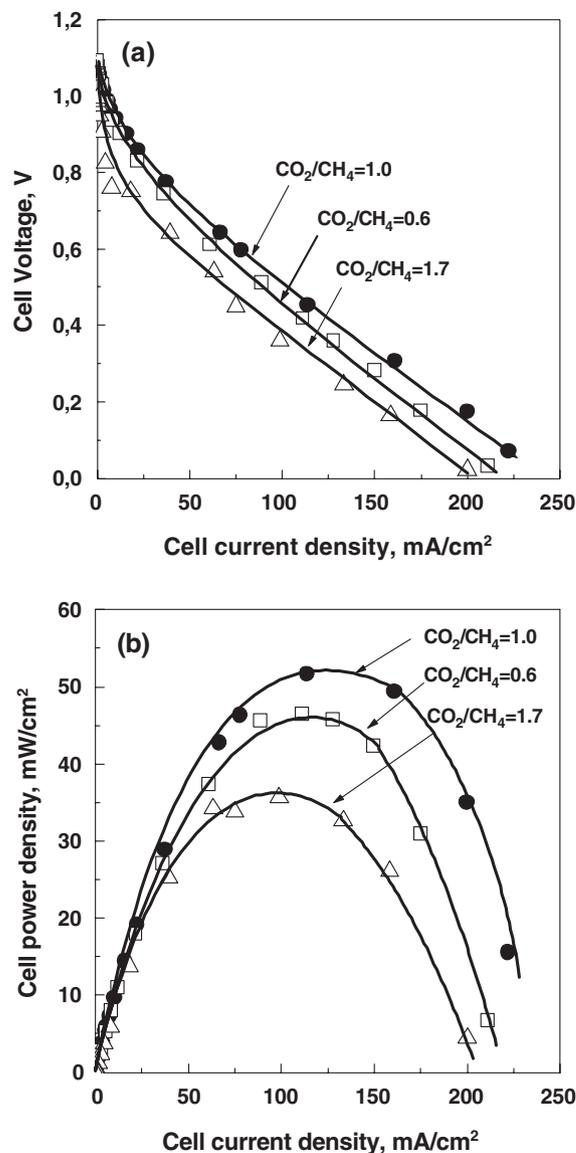
Fig. 3. Current–voltage (a) and current–power (b) behavior of the biogas fueled fuel cell under equimolar: 50% CO_2/50% CH_4, rich-quality: 36% CO_2/64% CH_4 and poor-quality: 63% CO_2/37% CH_4 biogas feed. Total flow rate F = 60 cm^3/min.

reaction (2) onto the anode results in maximization of the H_2 and CO concentrations at the anodic cell compartment. Since the charge transfer reactions (3) and (4) are related to the electrical energy produced by the cell, elevated concentrations of H_2 and CO are expected to have beneficial effects on the rates of these reaction steps and consequently on the electrical power generation, thus indicating the optimal conditions for fuel cell operation.

3.3. SOFC performance (closed-circuit data)

Fig. 3 shows typical voltage–current (Fig. 3a) and power output–current (Fig. 3b) closed-circuit data of the YSZ–SOFC operating at three different CO_2/CH_4 molar feed ratios. Since one of the principal limitations of biogas is its variability of quality, attention was given on the capability of the present fuel cell to

operate satisfactory under poor-quality biogas feed (i.e. low level of methane). As Fig. 3 shows, the constructed fuel cell operates satisfactorily for all three biogas compositions used. Cell current and power densities obtained have always the following decreasing order in respect to feed composition: equimolar biogas>rich-quality biogas>poor-quality biogas (Fig. 3). Maximum power output values of 51.6, 46.5 and 35.6 mW/cm^2 have been obtained for each case, respectively.

Data in Fig. 3a clearly show that ohmic polarization is not the only source of cell polarization; the slopes of the linear part of the V–i curves give, in a first approximation, the ohmic resistance of the cell, which is dominated by the resistance of the thick (1 mm) solid electrolyte component. All three cases indicate qualitatively similar ohmic resistances (parallel linear parts of the V–i curves). This implies that there are not changes in the chemical nature of the Ni-cermet electrode surface due to carbon deposition (at rich levels of CH_4) or Ni oxidation to NiO (at poor levels of CH_4) for the conditions used. Obviously, substantial improvements in power output can be obtained by using thinner YSZ components. The initial (low i) curvature of the V–i plots, slightly bigger in the case of poor-biogas feed (Fig. 3a), is mostly due to activation overpotential of the anodic and/or cathodic electrodes. Although the observed activation overpotentials are relatively low, their existence shows that the performance of our electrodes for the charge transfer reactions could be further optimized.

The power output of ∼50 mW/cm^2 obtained at 875 °C (Fig. 3b) is very encouraging considering the high thickness of our electrolyte wall of 1 mm. This value is compared favorably with other power density values of ∼60 mW/cm^2 reported in the literature for similar YSZ–SOFCs with a five times thinner electrolyte wall, i.e. 200 μm, operating at similar temperatures (850 °C) [11]. It is also interesting that biogas fueled fuel cell outputs taken are very close to or better than those measured when H_2 (40% in He) was fed to the cell at similar conditions.

One of the main problems very often addressed in the literature for the CO_2 or steam reforming of methane process over Ni catalysts is catalyst deactivation due to graphitic carbon deposition [4,5,9–16], while carbidic or adsorbed forms of carbon seem not to deactivate the catalyst because of their high reactivity with adsorbed O or O^{2-} species [15]. Methane cracking ($CH_4 \rightarrow C + 2H_2$) and Boudouard ($2CO \rightarrow C + CO_2$) reactions can occur onto the Ni–YSZ electrode to form carbon. However, cell operation under closed-circuit conditions is expected to prevent carbon deposition on the anode via the following electro-oxidation reactions:

$$C(s) + O^{2-} \rightarrow CO + 2e^- \tag{5}$$

$$C(s) + 2O^{2-} \rightarrow CO_2 + 4e^- \tag{6}$$
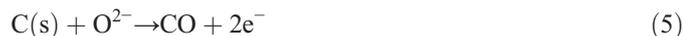
which also attribute, in parallel to reactions (3) and (4), to the cell electrical power generation. Indeed, recent studies on the internal CO_2-reforming of methane over NiO–MgO [10] and Ni–ScSZ [16] anodes in YSZ–SOFCs have shown that carbon deposition did not occur onto the anodes when the cells were operated under closed-circuit conditions. On the contrary, sufficient amounts of carbon on the anode surface were measured during open-circuit cell operation [10,16].

In order to examine the above described phenomena, long-term stability experiments were performed; our cell was operated for more than 3 days at the points of maximum power density for each of the three cases with different feed compositions used (Fig. 3b). Very stable operations were always recorded. In addition, after the end of each long-term experiment, no carbon was visibly observed on the anode. This practically implies that no accumulated carbon deposition is favored in our cell at closed-circuit conditions, and, even if it happens in micro-scale level, reactions (5) and (6) may occur preventing carbon deposition and attributing to the electricity production of the cell.

4. Conclusions

Generally speaking, our results showed that YSZ–SOFCs with Ni–YSZ cermet anodes can be successfully used as electrical energy production devices running directly on biogas fuel. Although equimolar CO_2/CH_4 feed ratio maximizes the rate of the dry internal reforming reaction of methane and consequently the electrical energy output characteristics of the SOFC, the cell was found to operate well and stably at a wide range of CO_2/CH_4 compositions, including poor-quality biogas. Carbon deposition onto the Ni-cermet anode was not visibly observed under closed-circuit operation of the cell; the cell operates very stably for a long period of time.

Acknowledgements

References

[1] J. Van herle, Y. Membrez, O. Bucheli, J. Power Sources 127 (2004) 300.
[2] M. Hammad, D. Badarneh, K. Tahboub, Energy Convers. Manag. 40 (1999) 1463.
[3] J. Huang, R.J. Crookes, Fuel 77 (1998) 1793.
[4] M.C.J. Bradford, M.A. Vannice, Catal. Rev., Sci. Eng. 41 (1999) 1.
[5] J.R. Nielsen, in: J. Anderson, et al., (Eds.), Catalysis Science and Technology, Springer-Verlag, 1983.
[6] M. Stoukides, Catal. Rev., Sci. Eng. 42 (2000) 1.
[7] I.V. Yentekakis, S. Neophytides, A. Kaloyannis, C.G. Vayenas, in: S.C. Singhal, H. Iwahara (Eds.), Proc. 3rd Int. Symp. SOFCs, The Electrochemical Society Inc., vol. 93-4, 1993, p. 904.
[8] T. Takeuchi, K. Yukimune, T. Yano, R. Kikuchi, K. Equchi, K. Tsujimoto, Y. Uchida, A. Ueno, K. Omoshiki, M. Aizawa, J. Power Sources 112 (2002) 588.
[9] N. Nakagawa, H. Sagara, K. Kato, J. Power Sources 92 (2001) 88.
[10] D.J. Moon, J.W. Ryu, Catal. Today 87 (2003) 255.
[11] J. Staniforth, K. Kendall, J. Power Sources 71 (1998) 275;
    J. Staniforth, K. Kendall, J. Power Sources 86 (2000) 401.
[12] D.G. Lamas, A. Ganeiro, D. Niebieskikwiat, R.D. Sanchez, D. Garcia, B. Alascio, J. Magn. Magn. Mater. 241 (2002) 207.
[13] Z. Zhang, X. Verykios, S. MacDonald, S. Affrossman, J. Phys. Chem. 100 (1996) 744.
[14] B.S. Liu, C.T. Au, Appl. Catal., A Gen. 244 (2003) 181.
[15] N.C. Triantafyllopoulos, S.G. Neophytides, J. Catal. 239 (2006) 187.
[16] A. Gunji, C. Wen, J. Otomo, T. Kobayashi, K. Ukai, Y. Mizutani, H. Takahashi, J. Power Sources 131 (2004) 285.